DIPOLE MOMENT OF QUASI-PLANAR BORON CLUSTERS

R. Becker [1], L. Chkhartishvili [2, 3]

[1] Cluster Sciences Research Institute
Boron Cluster Metamaterials
Ipswich, MA, USA
ionsourcerer@mac.com
[2] Department of Engineering Physics
Georgian Technical University
Tbilisi, Georgia
chkharti2003@yahoo.com
[3] Laboratory for Boron & Powdered Composite Materials
F. Tavadze Institute of Metallurgy & Materials Science
Tbilisi, Georgia

Accepted October 19, 2015

Abstract

Boron crystallizes in complex structures containing several non-equivalent atomic sites with different coordination numbers. Shifting of the electron density towards to the highly-coordinated atoms yields the palpable polarization of all-boron lattices, in general unexpected in elemental crystals. Same effect has to be inherent of boron clusters as well. We have experimental evidences that boron vapor consists of small clusters B_n, which are known to exhibit (quasi)planar structures (for number of boron atoms n not more than ~ 15). For all ground-state isomers of them we have estimated effective atomic charges and for asymmetric species – dipole moment as well. Binding energies per atom of (quasi)planar boron clusters, theoretically determined from the B–B interatomic pair potential, have been refined taking into account the obtained polarity of a part of B–B bonds.

Instead of introduction – An overeview

The role of boron in forming of the various structural phases, it is incommensurable of its abundance great. Understanding of the diversity of boron structures reduces to the electronic structure of an isolated boron atom. In multi-atomic networks, by the adding an electron the valence shell configuration peculiar to the free B atom $2s^2 2p$ transforms at first in the energetically more favorable configuration $2s^2 2p^2$, which then tends to most stable one $2s 2p^3$. Thus, boron is distinct electron-acceptor and, consequently, all-boron structures have to be electron-deficient. It is a reason why all the boron crystalline modifications exhibit complex – clustered structures. For them, the icosahedron B_{12} with 12 boron atoms at vertices serves as a main structural motif.

Since carbon nanosystems were discovered, it has triggered interest in other materials, including bare boron, which may also exhibit nanostructures. Boron-based nanomaterials are both of great academic and technological interests [1]. Due to its rich chemistry, boron is a natural choice for constructing nanosystems like the clusters, nanotubes, nanowires, etc. Relatively recently they were actually synthesized.

A boron atom of the given icosahedron is bonded with 5 neighboring atoms and, usually, is linked with an atom of the neighboring icosahedron. It explains why the average coordination number of atomic sites in all the solid-state forms of boron is almost 6. But, a free regular icosahedron B_{12} still remains electron-deficient: it needs 2 extra electrons to fill all the MOs (molecular orbitals). In boron crystals and amorphous boron, electron-deficiency is compensated by the presence of intrinsic point defects and / or certain impurity atoms in very high concentrations. In addition to solid-state modifications, constructed from full and fused icosahedra, elemental boron forms diboron molecule B_2 and molecular clusters B_n, $n > 2$. At relatively low n these clusters are (quasi)planar, but at sufficiently high n they can take polyhedral, nearly spherical, cage-like shapes and, in particular, icosahedral shape if dangling bonds at boron atoms are saturated by hydrogen or other foreign atoms. Thus, most boron atoms should be surrounded by 6 nearest neighbors, i.e. have 5 intra- plus 1 inter-icosahedral bonds. Alternatively, this circumstance leads to the possibility of synthesizing the fragments of (quasi)planar nanosheets in form of surfaces with triangular 6-coordinzted 2D lattices, which can be wrapped into nanotubes. Present 'Introduction' might be considered as a brief overview of the last decades' achievements in an important field of nano-structured boron – boron clusters.

As it is known, clusters as systems of a finite number of bound atoms are physical objects occupying an intermediate position between atomic particles (atoms and molecules) and macroscopic atomic systems (solids and liquids). One of the most interesting features of elemental boron is the occurrence of highly symmetric icosahedral clusters. However, the 5-fold symmetry does not lend B_{12} clusters to construct ideal 3D periodic frameworks, and various degrees of compromise in the pattern of icosahedral linkage give rise to the observed proliferation of boron polymorphs. Then, in bare boron structures most of the atoms usually are members of almost regular atomic triangles. This circumstance leads to possibility of the boron-based nanomaterials in form of (quasi)planar or convex boron surfaces with triangular 2D lattices. The rich chemistry of boron also is dominated by 3D cage structures. Consequently, it is important to gain deep insight in boron clusters – "building blocks" of nanoboron.

According to the mass-spectrometric analysis [2] of the boron cluster ions from the high-purity (99.99995 % B) target-source in process of growing of amorphous boron films, there are some peaks corresponding to the interval from B_2^+ to B_8^+.

Let start with diboron molecule B_2, the simplest boron cluster. The Douglas–Herzberg transition, observed [3] in the optical absorption spectrum of B_2, indicated that its ground electronic state is of Σ-type. In the other hand, the molecule B_2 was not observed via ESR (electron spin resonance), what was interpreted as support for the $^3\Sigma_g^-$ ground state rather than $^5\Sigma_u^-$ favored by ab initio calculations. Further more accurate CI (configuration interaction) calculation established [4] that the ground electronic state of B_2 indeed is of $^3\Sigma_g^-$ symmetry, and Douglas–Herzberg emission system is due to the transitions from the second $^3\Sigma_u^-$ state to the $X^3\Sigma_g^-$. Hyperfine coupling constants for the ground electronic state $^3\Sigma_g^-$ of the B_2 molecule were computed [5] using correlation procedures based on spin-unrestricted wave functions. As for

the potential curves, transition energies, and spectroscopic constants of several low-lying electronic states of the molecular ion B_2^+ and part of doubly excited states of B_2 were given in [6]. At the first time, a theoretical study of the IPs (ionization potentials) of the B_2 molecule was performed in [7]. An ab initio MO-study [8] of B_2 and B_2^+ determined the dissociation energy of the $^3\Sigma_g^-$ ground state of B_2 as 2.71 eV, and the adiabatic IPs to states $^2\Sigma_g^+$ and $^2\Pi_u$ of B_2^+ as 8.99 and 9.27 eV, respectively. The singlet, triplet, and quintet states of B_2 below about 45000 cm^{-1} were studied at the multi-reference CI level of the theory in an atomic natural orbital basis set [9]. The dissociation energy for the $X^3\Sigma_g^-$ state was computed to be 2.78 eV and estimated as 2.85 eV in the complete-CI limit. Calculations of excitation energies utilizing the standard coupled cluster hierarchy were presented [10] up to the quadruple excitation level for the open shell B_2 molecule using an excited closed shell state as a reference one.

Optimum geometries and harmonic spectra were obtained theoretically [11] for a number of different states of B_3 cluster. B_3 is found to be an equilateral triangle in its $2A'_1$ ground state. Estimated dissociation energy is 197.9 kcal / mole. From a statistical thermo-dynamical analysis, B_3 should be stable against dissociation to B_2 and B up to very high temperatures. Ab initio electronic structure calculations on several low-lying valence states of B_3 were also carried out using correlation-consistent polarized valence basis sets and SCF (self-consistent-field) treatments [12]. Stable triangular structures, linear structures, and Jahn–Teller unstable structures were also observed. The ground state of B_3 was predicted to have an equilateral triangular structure and to be of $^2A'_1$ symmetry in the D_{3h} point group. By carrying out a systematic basis set and electron correlation investigation, it was determined accurately the isotropic and anisotropic parts of the hyperfine coupling tensor of the B_3 molecule using the multi-CI SCF restricted–unrestricted method [13]. The spin polarization of the 1*s*-orbital on each B atom was found to be very small. This implies that in B_3 the isotropic hyperfine coupling is dominated by valence-orbital contributions rather than by 1*s*-orbital contributions.

The PES (potential energy surface) of B_4 cluster was ab initio studied using extended basis sets and coupled cluster methods [14]. The ground state $^1A_{1g}$ is the singlet square that undergoes pseudo Jahn–Teller distortion to a rhombic structure ^1A_g, but the energy gain is too small. Total atomization energies of B_2, B_3, and B_4 clusters were computed as 62.2, 189.1 – 192.6, and 312.2 kcal / mole, respectively. The two small boron clusters B_3 and B_4 in their neutral and anionic forms were studied by photoelectron spectroscopy and ab initio calculations [15]. Vibrationally resolved photoelectron spectra were observed for B_3^- at 355, 266, and 193 nm, and the EA (electron affinity) of B_3 was measured to be 2.82 eV. An unusually intense peak due to two-electron transitions was observed in the 193 nm-spectrum of B_3^- at 4.55 eV. It was confirmed that both B_3^- and B_3 are of D_{3h} symmetry. The photoelectron spectra of B_4^- were also obtained at the three photon energies, but much broader spectra were observed. The B_3^- anion was found to have the lowest electron detachment energy, 1.6 eV, among all boron clusters with more than three atoms, consistent with its extremely weak mass-signals. The neutral B_4 cluster was found to have a D_{2h} rhombus structure, which is only slightly distorted from a perfect square. For B_4^-, it was identified computationally two low-lying isomers $^2B_{1u}$ and ^2A_g, both of D_{2h} symmetry, with the slightly more stable $^2B_{1u}$ state.

The electronic structure and chemical bonding of boron clusters B_5 and B_5^- were investigated [16] using anion photoelectron spectroscopy and ab initio calculations. Extensive searches were carried out for global minimum of B_5^-, which was found to have a planar structure with a closed-shell ground-state. Excellent agreement was observed between ab initio

detachment energies and the experimental spectra. A bonding orbital was found to be completely delocalized over all 5 atoms in the B_5^-. Such bonding makes B_5^- more rigid towards butterfly out-of-plane distortions. The structure and stability of B_5, B_5^+ and B_5^- clusters were investigated theoretically also in [17]. Eight B_5, seven B_5^+, and seven B_5^- isomers were identified. The planar 5-membered ring structures, B_5 and B_5^+, were found to be the most stable on the neutral and cationic PES, respectively. The most stable B_5^- isomer has an arrangement of atoms similar to the neutral. Natural bond orbital analysis suggests that there are 3-centered bonds in both the neutral and anionic structures, as well as the multi-centered centripetal bond in the cationic structure.

The electronic structure and chemical bonding of B_6 and B_6^- clusters were investigated using anion photoelectron spectroscopy and ab initio calculation [18]. The global minimum of B_6^- has a doublet ground state. The corresponding ground-state structure of B_6^- is planar. The chemical bonding in B_6^- can be interpreted in terms of linear combinations of MOs of two B_3^- fragments. The antiaromatic nature of chemical bonding was established for both B_6^- and B_6^{2-}. Electronic structure, isomerism, and chemical bonding in B_7^- and B_7 clusters were studied in [19]. The structures of B_7, B_{10} and B_{13} boron clusters were studied [20] using the FP (full-potential) LMTO (linear-muffin-tin-orbitals) MD (molecular dynamics) method. Seven stable structures for B_7 and fifteen for B_{10} were obtained. C_{2h}–B_{10} is the most stable among the 15 structures, but C_{2v}–B_{10} is not stable. For B_{13}, three degenerate ground-state structures were found. The potential surface near C_{2v}–B_7 (ground state) and D_{6h}–B_7 is very flat. As a fundamental unit in constructing bigger clusters, C_{2v}–B_7 will change its form easily. The most stable structures for B_7, B_{10} and B_{13} clusters are two-dimensional (quasi)planar clusters, rather than the three-dimensional ones.

Probes of bonding in small boron clusters B_{2-8}^+ performed by the measurements of threshold energies and fragmentation patterns for collision-induced dissociation showed [21] that primary fragmentation channel is loss of B^+ in all cases and B_5^+ is a particularly abundant cluster in the distribution produced. The stabilities of B_n clusters with $4 \le n \le 8$ based on the vibrational analysis were investigated by ab initio MO-calculations in [22]. It was found that there exist two types of stable clusters: a low-symmetry, structurally "soft", species with lower frequencies and lower geometrical change barriers and a high-symmetry, structurally "hard", species with higher frequencies. By means of ab initio techniques, the equilibrium geometries, total, binding and fragmentation energies of clusters B_n, with $n = 2-8$ were calculated both in the neutral and cationic states in [23]. The experimental and theoretical evidence that 8- and 9-atom boron clusters are perfectly planar molecular wheels, with a hepta- or octa-coordinated central boron atom, respectively, were reported in [24]. DFT (density functional theory) calculations using a PW (plane wave) basis set and a PP (pseudopotential) were employed [25] to investigate the structure, vibrational characteristics, and energetics of small (up to 10 atoms) boron clusters. Comparison with other studies revealed a great deal of consensus about the most stable structures for B_2, B_3, B_4, B_7, and B_8, and maybe B_5 as well. Additionally, all studies agree about the existence of two stable B_6 isomers.

Geometries, electronic structures and energies of the neutral and cationic clusters B_{2-12} and B_{2-12}^+ were investigated by the ab initio MO method [26]. The geometries of boron-cluster cations B_{3-12}^+ are essentially the same as those of the neutral clusters – the (pseudo)planar cyclic structures. Clusters of 8–11 atoms characteristically have the most stable structure of a cyclic form with 1 atom in the middle. The capped pentagonal B_6, B_7 and B_7^+ and the trigonal

bipyramidal B_{12} and B_{12}^+ seem to be the exceptions. The electronic and geometric structures, total and binding energies, harmonic frequencies, point symmetries, and HOMO–LUMO (highest occupied MO–lowest unoccupied MO) gaps of small neutral boron B_n clusters ($n = 2-12$) were investigated in [27] using DFT. Linear, (quasi)planar, open- and 3D-cage structures were found. None of the lowest energy structures and their isomers has an inner atom. Within the size range, the (quasi)planar, i.e. convex, structures have the lowest energies.

It is expedient to consider boron icosahedron B_{12} separately from other boron clusters. At the first time, the electron structure of a regular icosahedron of boron atoms was investigated [28] theoretically by the method of MOs. It was found that 30 bonding orbitals are available for holding the icosahedron together, besides the 12 outward-pointed equivalent orbitals of the separated atoms. In [29], the energy spectrum of a real boron icosahedron – unit cell of the α-rhombohedral boron crystal – was studied using MO–LCAO (linear-combinations-of-atomic-orbitals) method. It is an electron-deficient structure. Besides, in distorted in crystalline field icosahedron the bond lengths are different and now there is no 5-fold symmetry axis. It was found that molecular levels placed at –9.35 eV should be half-filled, while all lower energy levels should be filled. Using a PW expansion, it was performed [30] ab initio calculations of the energy bands, equilibrium structural parameters, atomic positions, and cohesive energy of boron icosahedron B_{12}. As for the calculated charge-density contour plots, they revealed strong intra-icosahedral bonding. Based on the group properties of a regular icosahedron, its normal vibrational modes were pictured [31]. There are 8 distinct frequencies for the 30 normal modes with 1-, 3-, 4-, and 5-fold degeneracies. Icosahedral oscillations can be pictured in terms of three equilibrium descriptions: the first involves 2 parallel regular pentagons and 2 polar atoms; the second has 2 polar triangles and 1 equatorial puckered hexagon; while the third consists of 6 pairs of atoms on opposite faces of a cube. It was shown [32] that by the interaction between electron and pair of phonons, which are the slightly modified 2 breathing modes of the isolated icosahedron B_{12}, an electron trapping level generates in icosahedral boron-rich solids. The polar vibrations for the B_{12} icosahedron were demonstrated [33] within the harmonic approximation by using the shell model. The tensor nature of dynamical effective charges was emphasized. It was shown that the effective charge of the regular B_{12} is very small ($\approx 0.01e$), while that of α-rhombohedral boron unit cell is enhanced by the deformation. The covalent-to-metallic bonding conversion in boron icosahedral cluster solids was discussed [34] in relation to the occupation by an atom the center of this cluster. The corresponding change in the electron localization was quantitatively estimated by using ELI (electron localization indicator). Namely, the distributions of the ELI were compared for the pair of clusters B_{12}^+ and B_{13}^-. This comparison revealed that the bonding conversion from covalent to metallic one involves a decrease in both the electron-density and ELI between boron atoms.

Bonding of small boron cluster cations from B_2^+ to B_{13}^+ was examined [35, 36] by measurements of appearance potentials and fragmentations patterns for collision-induced dissociation. Cluster stabilities were generally found to increase with increasing size. The lowest energy fragmentation channel for all size cluster ions is loss of a single B atom. Clusters, smaller than 6 atoms, preferentially lose B^+ ion, while for larger clusters the charge remains on the B_{n-1}^+ fragment. Electronic and geometric isomers of B_{13} clusters were calculated within the LDA (local density approximation) [37]. The filled icosahedral structure was found unstable. While heating and slow cooling lead to a considerably more stable (by 0.68 eV) structure with high

symmetry (C_{3v}) and coordination. The remarkable stability of this isomer may explain the measured high survival of B_{13}^+ clusters on collision and its relatively low reactivity. Analogous problem was considered [38] for the neutral and cationic clusters B_{12} and B_{13}. Several planar and non-planar stationary structures were optimized for neutrals and cations of each cluster size. A characteristic cyclic form with 1 atom in the middle was found to be stable for each cluster, while the icosahedral B_{12}^+ was found to be the most stable. The triplet icosahedral state was found to be stable, but energetically unfavorable than the cyclic B_{12}. The structures and energies of B_{13}^+, observed experimentally to be an unusually abundant species among cationic boron clusters, were studied systematically with DFT in [39]. The most thermodynamically stable B_{12}^+ and B_{13}^+ clusters are confirmed to have (quasi)planar rather than globular structures. However, the computed dissociation energies of the 3D B_{13}^+ clusters are much closer to the experimental values than those of the (quasi)planar structures. Hence, planar and 3D B_{13}^+ may both exist. The curiously stable cationic B_{13}^+ cluster and its neutral and anionic counterparts were examined in [40] though the use of DFT. While no minima that corresponded to the filled icosahedron could be found for the cluster, an intriguing atom-in-cage structure was found that is a local minimum on the cationic, neutral, and anionic surfaces. In the structure found for the B_{13}^- anionic cluster, the 12 external boron atoms are arranged as 3 of 6-membered rings back-to-back. The (quasi)planar structures are seen to be more stable than 3D isomers, but their ordering by stability changes depending on the charge state. It was found that planar structures benefit from π-delocalization and in the case of the global minimum of the B_{13}^+ cationic cluster this delocalization is reminiscent of aromaticity. As it was postulated, the lowest-energy B_{13}^+ isomer proved to be highly aromatic. The topological resonance energy of this cationic boron cluster is positive in sign and very large in magnitude. This constitutes the definitive reason why B_{13}^+ is kinetically stable and (quasi)planar in geometry [41]. The electron-deficient and multivalent character of boron is responsible for the high aromaticity of this cluster. In addition, its minimum bond resonance energy is not too small. Some of thermo-chemical parameters of a set of small-sized neutral B_n and anionic B_n^- boron clusters, with $n = 5-13$, were determined using coupled-cluster theory calculations [42]. Enthalpies of formation, adiabatic electron EAs were evaluated in good agreement with experiments (values are given in eV): B_5 (2.29 – 2.48 and 2.33), B_6 (2.59 – 3.23 and 3.01), B_7 (2.62 – 2.67 and 2.55), B_8 (3.02 – 3.11 and 3.02), B_9 (3.03 and 3.39), B_{10} (2.85 and 2.88), B_{11} (3.48 and 3.43), B_{12} (2.33 and 2.21), and B_{13} (3.62 and 3.78). The calculated adiabatic detachment energies to the excited states of B_6, which have geometries similar to the state of B_6^-, are 2.93 and 3.06 eV, in excellent agreement with experiment. Based on the ab initio QC (quantum chemical) methods, fragmentation channels, IPs, and the Coulomb explosion of multi-charged boron clusters B_n ($n = 2-13$), were determined [43]. The electron-deficient boron clusters sustain more stability and hardly fragment when they are negatively charged. Stability of boron clusters decreases with increasing ionization. Only by the first ionization the odd-size clusters are more stable than the even-size clusters. Further ionizations cause the repulsive Coulomb force between the constituent atoms to get stronger, and lead first to metastable states, then to the Coulomb explosion of clusters. None of the cationic boron clusters studied remains stable after 6 times ionization. The critical charge for metastability was estimated as $Q_m \le n/2$ for even-size clusters, and $Q_m \le (n-1)/2$ for odd-size clusters. In addition, the critical charge for the Coulomb explosion is found to be $Q_c \le n/2+1$ and $Q_c \le (n+1)/2$, respectively. Several dissociation channels of B_n^+ and B_{13}^Q isomers with the

lowest fragmentation energies were presented. All of the vibrational frequencies were found positive indicating that no transition state is possible for the clusters studied.

The structures of B_{14} and B_{14}^{2-} in octahedral symmetry were investigated by ab initio calculations [44]. The geometrical structures and properties of small cationic boron clusters B_n^+ ($n = 2-14$) were determined [45] using the LSD formalism. Most of the final structures of the cationic boron clusters prefer (quasi)planar arrangements and can be considered as fragments of a planar surface or as segments of a sphere. The calculated adiabatic IPs of B_n exhibit features similar to those of measured IPs. Most of the calculated normal modes of the cationic clusters have frequencies around 1000 cm^{-1} and strong IR (infrared) intensities. A linear search for minima on PESs based on analytical gradient methods and the determination of binding energies of small boron clusters B_n ($n = 2-14$) were conducted using the ab initio HF (Hartree–Fock), and SCF CI and QC methods, as well as by means of DFT at the levels of LSD and non-local corrections to the exchange-correlation functional [46, 47]. The final optimized HF-topologies of the neutral boron clusters are identical with those derived with the LSD approximation. The most stable boron clusters have convex or (quasi)planar structures and the convex clusters seem to be segments of the surface of a sphere. The geometries of B_n^+ clusters for $n \leq 14$ were optimized in [48] applying DFT. The calculation suggested that the experimental results for the $B_n^+ \rightarrow B^+ + B_{n-1}$ fragmentation energies are too small, while experimental $B_n^+ \rightarrow B + B_{n-1}^+$ fragmentation energies for B_4^+, B_5^+, and B_{13}^+ are too large. Then, the fragmentation energies were calibrated based on coupling cluster theory. Overall corrected fragmentation energies are found to be in reasonable agreement with experiment. The most stable structure for each cluster was found to be (quasi)planar. The larger clusters are derived from fusing 6- and / or 7-membered atomic rings, which share 4 atoms for the 6 – 6 and 6 – 7 rings and 5 atoms for the 7 – 7 rings. Based on ab initio DFT and QC methods, accurate calculations on small boron clusters B_n ($n = 2-14$) were carried out in [49 – 51] to determine their electronic and geometric structures. Most of these final structures with $n > 9$ are composed of two fundamental units: either of hexagonal or pentagonal pyramids different from the classical forms of crystalline boron. Using "Aufbau principle", one can easily construct various very stable boron species. The resulting (quasi)planar and convex structures can be considered as fragments of planar surfaces and segments of nanotubes or hollow spheres, respectively.

Above a certain size, boron clusters prefer a cylindrical arrangement over a planar one. Experimental determination of the collision cross section combined with DFT calculations showed [52] that the transition to cylindrical structures takes place at B_{16}^+. The structure and chemical bonding of B_{16}^- were studied [53] using ab initio calculations and photoelectron spectroscopy. Its global minimum is found to be a (quasi)planar and elongated C_{2h}-structure. Addition of an electron to B_{16}^- resulted in a perfectly planar and closed shell B_{16}^{2-} (D_{2h}).

Photoelectron spectroscopy reveals a relatively simple spectrum for B_{19}^-, with a high electron-binding energy [54]. Theoretical calculations show that the global minimum of B_{19}^- is a nearly circular planar structure with a central B_6 pentagonal unit bonded to an outer B_{13} ring.

Experimental studies and computational simulations revealed [55] that boron clusters, which favor 2D structures up to 18 atoms, prefer 3D structures beginning at 20 atoms. Using global optimization methods, it was found that the B_{20} neutral cluster has a double-ring tubular structure with diameter of ~ 5.2 Å. For the B_{20}^- anion, the tubular structure is shown to be isoenergetic to 2D structures, which were observed and confirmed by photoelectron

spectroscopy. The 2D-to-3D structural transition observed at B_{20} suggests that it may be considered as the embryo of the thinnest single-walled boron nanotubes. B_n^- cluster anions were produced by laser vaporization of a target made of enriched ^{10}B isotope in the presence of the He carrier gas and analyzed with TOF (time-of-flight) mass-spectrometer. High-level ab initio MO methods were employed [56] to determine the relative stability among four neutral and anionic B_{20} isomers, particularly, the double-ring tubular isomer versus three low-lying planar isomers. They also suggest that the planar-to-tubular structural transition starts at B_{20} for neutral clusters but should occur beyond the size of B_{20}^- for the anion clusters. In order to elaborate a direct experimental method available for structural determination of boron clusters, photoelectron spectroscopy of size-selected cluster anions was combined with quantum calculations to probe the atomic and electronic structures and chemical bonding of small boron clusters up to 20 atoms [57]. Based on this method the experimental and theoretical evidences were presented showing that small boron clusters prefer planar structures and exhibit aromaticity and antiaromaticity according to the Huckel rules. Aromatic boron clusters possess more circular shapes whereas antiaromatic ones are elongated. It was found that for neutral boron clusters the planar-to-3D structural transition occurs at B_{20}, which possesses a double-ring structure, even though the B_{20}^- anion remains planar.

Based on a series of ab initio studies [58] had pointed out the remarkable structural stability quasi-planar boron clusters, and postulated the existence of novel layered boron solids built from elemental subunits. The equilibrium geometries and the systematics of bonding in various isomers of a 24-atom boron cluster was investigated [59] using Born–Oppenheimer MD within the framework of DFT. The B_{24} isomers studied were the rings, convex and (quasi)planar structures, the tubes, and closed structures. A staggered double ring is found to be the most stable structure among these isomers. Using ab initio QC methods, different structures of B_{32} clusters was investigated in [60]. The most stable isomers have (quasi)planar or tubular structures often containing dove-tailed hexagonal pyramids. In contrast, hollow spheres are less stable. Their stability can be understood as a competition between a curvature strain (favoring (quasi)planar clusters) and elimination of dangling bonds (favoring tubular and cage structures).

The boron clusters B_n, $n = 2-52$, formed by laser ablation of hexagonal boron nitride were discovered with a TOF mass-spectrometer [61]. Using ab initio QC and DFT methods, it was investigated the structural transition from planar 2D boron clusters into 3D double-ring system and then into triple-ring system [62]. The first structural transition occurs at B_{19} and B_{20} clusters, while the second transition occurs between B_{52} and B_{54} clusters. The effect of the repulsive Coulomb forces in boron clusters when they are multi-ionized also was studied. A mass spectrometric study of boron cluster anions B_n^-, $n = 7-55$, produced by laser vaporization from two different types of boron-containing sample rods: boron-rich boride and pure boron, was reported in [63]. In mass spectra recorded from the boride sample, a repeating intensity pattern of boron cluster anions having local maxima at $(B_{13}^-)(B_{12})_{0,2,3}$ as well as at B_{26}^- was observed. Similar phenomena were not observed with a pure boron sample. These facts were attributed to the structural differences between the two materials, in particular, $(B_{12})(B_{12})_{12}$ super-icosahedral structure characteristic of the crystalline boron-rich borides.

And finally, let refer to some studies considering the issue of boron clusters. Some symmetrical clusters of boron, and carbon as well, were discussed [64] by introducing the concept of conjugate polyhedra. It was concluded that if a polyhedron of carbon is given, its conjugate polyhedron of boron can be obtained and the conjugate polyhedron should be of

same symmetry. Based on ab initio QC and HF approximations, and DFT and LMTO methods within the ASA (atomic-sphere-approximation) in [65] the geometric and electronic structures of some atomic-scaled boron clusters were determined. In [66], there were reported experimental and theoretical evidences that small boron clusters prefer planar structures and exhibit aromaticity and antiaromaticity according to the Huckel rules. The planarity of the species was further elucidated on the basis of multiple aromaticity and antiaromaticity, and conflicting aromaticity. The major aims of the current research in field of boron clusters, which are developing, simulating, modeling, and predicting new boron structures to build pre-selected, uniform nanostructural materials with specific properties, e.g. superhardness, superconductivity, superlightness, and propellance, were formulated in the review [67]. According to these and other results obtained by Boustani and co-workers, one can conclude that most structures of boron clusters can be classified into four groups: (quasi)planar, tubular, convex, and spherical clusters. The transition of the (quasi)planar surfaces into tubules may be pictured by rolling the surfaces and forming cylinders. The closure of boron (quasi)planar surfaces into tubules goes through an energy barrier path. Small boron clusters as individual species in the gas phase were reviewed in [68]. Free boron clusters were characterized using photoelectron spectroscopy and ab initio calculations, which have established the (quasi)planar shapes of small boron clusters for the first time.

Recently, it was experimentally detected [69] the highly stable quasi-planar boron cluster B_{36} of hexagonal shape with the central hexagonal hole.

Boron vapor – Experimental part

There are evidences [70 – 72] that liquid boron consists not of icosahedra, but mainly (quasi)planar clusters. Ab initio MD simulations of the liquid boron structure yields that at short length scales icosahedra B_{12}, a main structural motif of boron crystals and boron-rich compounds, are destroyed upon melting although atoms form an open packing with still 6-coordination, i.e., the structure of liquid boron is similar to the boron non-icosahedral forms. According to measurements of the structure factor and the pair distribution function, process of melting is associated with relatively small changes in short-range order of the system. Results of a comprehensive study of liquid boron atomic structure with X-ray measurements coupled with ab initio MD simulations also show that there is no evidence of survival of the icosahedral arrangements into the liquid, but many atoms appear to adopt a geometry corresponding to the quasi-planar pyramids.

We can conclude that, during melting of boron it takes place the boron clusters emission and thus boron vapor formed have to consist of mainly from boron clusters.

We developed [73] a method of generating substantially pure boron cluster-ions by a heating within a suitable temperature range the boron-rich material electrode, which induces its controlled thermal decomposition in a stoichiometrically favorable manner – providing boron vapor and all other species not in the vapor state. Magnetic confinement of the released electrons causes collisions resulting in ionization of the vapor to the plasma state. This plasma may then be extracted and accelerated at the suitable energy, e.g. toward a work-piece for use as a plasma-process feed gas.

Such a method of coating by boron has a variety of applications, including surface chemical and wear protection, neutron absorption, prevention of impurity emission from

heated filaments and ion beams, elimination of metal dust from vacuum systems, boridizing, reactive chemistry, etc.

Using the method of plasma spray, boron can be deposited onto most metals and a wide variety of ceramics and insulators including boron nitride BN and quartz. Adhesion of boron coatings to these materials is particularly strong. In this work, a high electric current (of 75 A) has been drawn between two graphite electrodes connected by an electrically conductive boron-rich boride powder (the thickness of powder separating the electrodes has been up to 2.5 cm) while in vacuum. The powder was observed to melt and begin emitting boron vapor, which was used to coat a glass slide test sample. A high coating rate of over 0.003 in. / min at a distance of 2 in. from the evaporation source was observed.

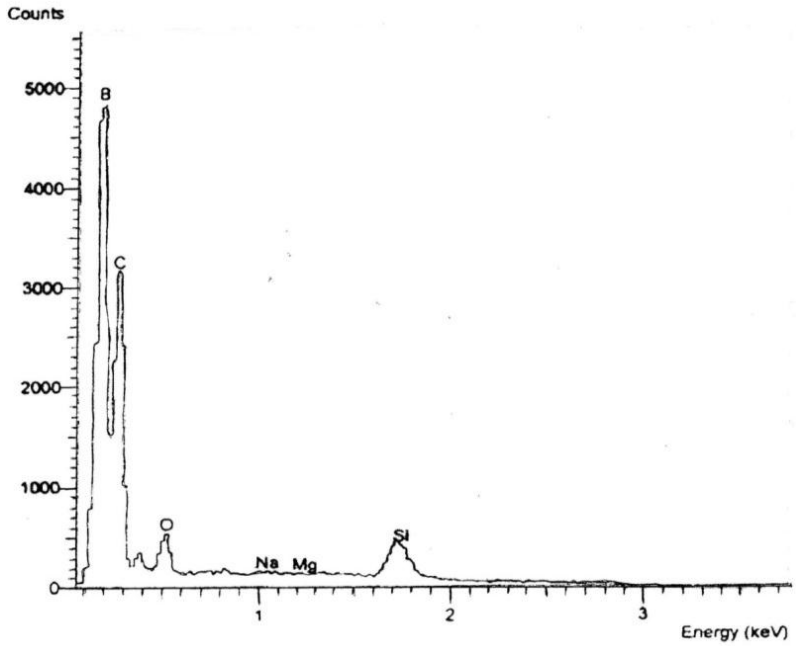

Figure 1. EDAX Measurement of coating produced onto a glass slide.

Figure 1 shows an EDAX analysis (energy dispersive analysis by X-ray) of the resultant coating material. The peak at the far left is due to boron coating. The other peaks are from the glass substrate. As is known, EDAX is low-sensitive to light elements, such as boron. It is a reason why the boron peak observed in the mass spectrum appears unnaturally small compared to the background elements from the glass slide substrate.

In the process of melting and evaporation of a boron-rich material with the nitrogen source in form of high-purity pressed boron nitride rods, the shell structures of chemical composition BN_x with boron excess ($x << 1$) contaminated with carbon has been synthesized [74]. The obtained material is conductive despite the fact that all the boron nitrides of stoichiometric chemical composition BN are insulators. "Metallic" boron nitride is modeled as a mixture of structural modifications of semiconducting boron and boron carbide heavily doped with nitrogen [75].

Previously, we reported (see [63]) a mass spectrometric study of boron cluster anions B_n^-, $n = 7-55$, including the heavier species containing B_{12}-icosahedra, which were produced by laser vaporization both from pure boron (i.e. homogeneous) and boride (i.e. heterogeneous) target rods. While at lower masses these spectra were similar, at higher masses the boride spectrum exhibited a completely different pattern: in addition to the local maximum at B_{13}^-,

characteristic of the pure boron spectrum as well, a repeating intensity pattern having two additional local maxima were observed. These observations can be attributed to the structural differences between the two target materials. Further, we had demonstrated [76] that created boron clusters can be self-assembled into nanostructures.

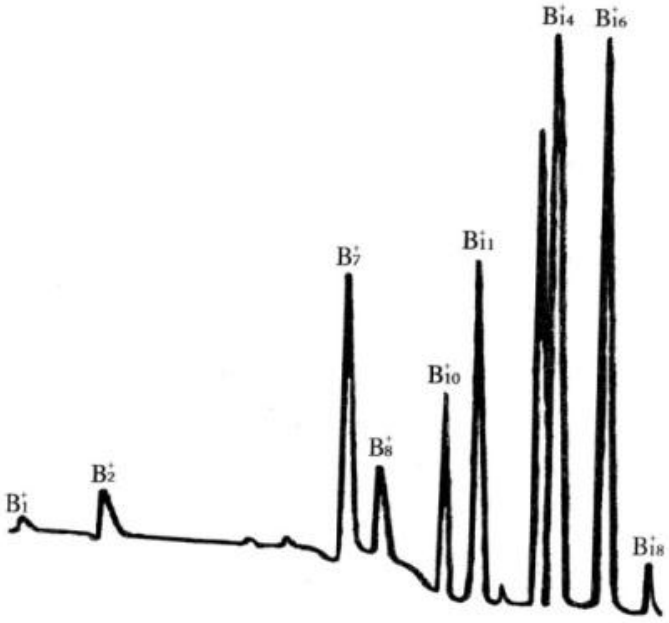

Figure 2. Mass spectra of boron cluster cations generated by the thermal vaporization of: a boron-rich material.

From the mass spectra of small boron cluster anions generated by the laser vaporization, one can see that main maximum is placed within the range B_{11} – B_{13} (see [63]). The mass spectrum of small boron cluster cations generated by the thermal vaporization in present work is shown in **Figure 2**. The spectrum shape is similar, unless main maximum is shifted in the range B_{14} – B_{16}.

Binding energy taking into account atomic charges and dipole moment – Teorizing

From the review given into Introduction, we can assume that, at the sufficiently low number of atoms *n* formation of the 3D clusters are not preferable kinetically, even that is preferable energetically, i.e. because of higher binding energy per atom. The 2D – (quasi)planar – structures built up from boron atoms, seem to be preferable because they are open for further adding of atoms to realize B atoms' ability to bound up to 6 other boron atoms in the cluster's plane.

However, small boron clusters would be quasi-planar, not ideally planar. Due to clusters' finite sizes: atoms at the periphery have fewer neighboring atoms, i.e. possess lower coordination numbers, than their counterparts placed at the central part. It leads to the formation of bonds with unequal lengths and then distortion of a structure consisting of only regular triangles with B atoms at the vertices. This is a reason why small boron clusters are not ideally planar, but buckled and / or puckered.

When number of atoms *n* becomes sufficiently high, the saturation of all the 6 potentially possible bonds of a boron atom can be achieved by the alternative way – by

wrapping of the plane into a cylinder (i.e. boron nanotube) or sphere (i.e. boron fullerene). But, these processes result in formation of 3D structures. The cluster B_{21} serves for the embryo of small boron nanotubes. Thus, here we consider boron (quasi)planar clusters with number of constituting atoms up to ~ 15. The clusters with high n possess several isomers. We will analyze only one of them – most stable, usually, with highest number of B–B bonds and symmetric.

On the basis of quasi-classical theory of substance [77], the B–B interatomic pair potential was constructed [78, 79] within the initial quasi-classical approximation. This potential was successfully exploited in calculations of binding energies of all-boron nanostructures [80 – 83], as well as some boron-isotopic effects in boron-rich solids [84 – 88]. According to the quasi-classical B–B pair potential, the binding energy of $\varepsilon_b \approx 2.80$ eV corresponds the equilibrium interatomic distance (B–B pair bond length) of $l_b \approx 1.78$ Å. Below these values are used for estimating binding energy of small boron clusters.

For further consideration we also need to introduce atomic units (a.u.) of energy, length and electric dipole moment respectively, $E_{\text{a.u.}} \approx 27.212$ eV, $l_{\text{a.u.}} \approx 0.52918$ Å and $p_{\text{a.u.}} \approx 2.5417$ Dy. And finally, let's $N = 1,\ldots,n$ numbers atoms constituting the (quasi)planar boron cluster B_n, C_N is the coordination number of the corresponding boron atom in this structure, and v is the atoms' valence – number of the valence electrons. As is known, for boron atom $v = 3$. In the **Table 1** shown below, boron atoms constituting small cluster are denoted as $N[C_N]$.

Effective atomic charges and dipole moment

In average, an atom utilizes v/C_N electrons per bond for bounding with nearest neighbors (because boron clusters like other all-boron structures are electron-deficient, effective numbers of bounding electrons mostly could be fractions, lesser than 1). The N-atom in average a half of these electrons, $v/2C_N$, transfers to each of neighboring atoms. It is clear that, for any atom in average the total number of transferred electrons is same, $v/2$. From their side, neighboring atoms transfer a part of their valence electrons to the N-atom. Net number of transferred and received electrons determines the effective charge number for each atom constituting a cluster.

Atoms of the central part are highly-coordinated. Thus, they receive more electron charge than transfer, and could be charged negatively. On contrary, atoms at the periphery receive lesser electrons than transfer, and could be charged positively.

When a cluster shapes itself asymmetrically, it possesses a non-zero dipole moment, value of which can be calculated from the standard relation

$$p = e\left|\sum_{N=1}^{N=n} Z_N \vec{r}_N\right|, \qquad (1)$$

where $\vec{r}_N$ denote radius-vectors of atomic sites in the cluster, and Z_N is the effective charge number of the N-atom. When calculating $\vec{r}_N$, we can neglect by the changes in bond length assuming it being same as in non-distorted ideally planar structure. As mentioned, within the quasi-classical approximation $l_b \approx 1.78$ Å and, consequently, $el_b \approx 8.55$ Dy.

Planar images of the clusters considered and their calculated dipole moment are shown below in the **Table 1**.

Table 1. Structure, dipole moment and binding energy of small boron clusters.

B_n	Structure	Binding energy E_b, eV / atom		Dipole moment p, Dy	
		Formula	Value	Formula	Value
B_1		0	0	0	0
B_2		$\frac{\varepsilon_b}{2}$	1.40	0	0
B_3		ε_b	2.80	0	0
B_4		$\frac{5\varepsilon_b}{4}+\frac{3\varepsilon_e}{16}$	5.02	0	0
B_5		$\frac{7\varepsilon_b}{5}+\frac{73\varepsilon_e}{320}$	5.77	$\frac{\sqrt{3}el_b}{8}$	1.85
B_6	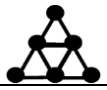	$\frac{3\varepsilon_b}{2}+\frac{9\varepsilon_e}{32}$	6.48	0	0
B_7	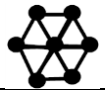	$\frac{12\varepsilon_b}{7}+\frac{15\varepsilon_e}{56}$	6.97	0	0
B_8		$\frac{13\varepsilon_b}{8}+\frac{729\varepsilon_e}{3200}$	6.39	0	0
B_9	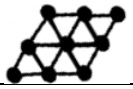	$\frac{16\varepsilon_b}{9}+\frac{35\varepsilon_e}{288}$	5.96	0	0
B_{10}	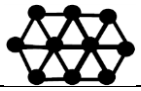	$\frac{19\varepsilon_b}{10}+\frac{7\varepsilon_e}{80}$	6.03	0	0
B_{11}	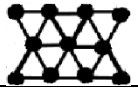	$\frac{20\varepsilon_b}{11}+\frac{1197\varepsilon_e}{8800}$	6.19	0	0
B_{12}	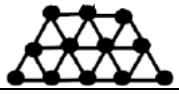	$\frac{23\varepsilon_b}{12}+\frac{7\varepsilon_e}{96}$	5.96	$\frac{\sqrt{3}el_b}{8}$	1.85
B_{13}	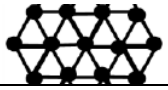	$2\varepsilon_b+\frac{37\varepsilon_e}{416}$	6.32	0	0
B_{14}	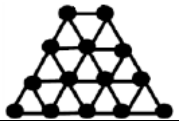	$2\varepsilon_b+\frac{13\varepsilon_e}{896}$	5.72	$\frac{\sqrt{3}el_b}{8}$	1.85
B_{15}	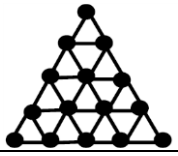	$2\varepsilon_b+\frac{\varepsilon_e}{24}$	5.94	0	0

Relative stability

To estimate relative probabilities of formation of (quasi) planar boron clusters B_n, $n = 1,2,3,\ldots$, we need to start from the estimation of their relative stabilities, i.e. binding energies per atom.

Initially, binding energy per atom can be estimated in a "tight-binding" approximation, i.e. taking into account only interactions between nearest neighboring atoms:

$$E_{b0} = \frac{\varepsilon_b}{2n}\sum_{N=1}^{N=n} C_N , \qquad (2)$$

where $\varepsilon_b / 2$ is the binding energy per a B atom bounded with another B-atom. As mentioned, in the quasi-classical approximation, the numerical value of the parameter ε_b is about 2.80 eV.

The N -atom's binding energy correction related to the its electrostatic (Coulomb) interaction with neighboring N'-atom with effective charge number of $Z_{N'}$ in eV equals to $-Z_N Z_{N'} \varepsilon_e / 2$, where $\varepsilon_e = E_{\text{a.u.}} l_{\text{a.u.}} / l_b$ is the energy parameter inversely proportional to the bond length. Here, we again can neglect by the changes in bond length assuming l_b to be of 1.78 Å within the initial quasi-classical approximation. It means that $\varepsilon_e \approx 8.09$ eV. By the introducing the factor 2 in the numerator, we take into account that same correction should be attributed to the counterpart N'-atom as well. Thus, correction to the binding energy per atom related to the effective atomic charges is

$$E_e = -\frac{\varepsilon_e}{2n}\sum_{N=1}^{N=n} Z_N \sum_{N'=1}^{N'=C_N} Z_{N'} . \qquad (3)$$

When $Z_N Z_{N'} < 0$, the pair of atoms are attracted each by other and binding energy increases. But, when $Z_N Z_{N'} > 0$, they are repulsed and binding energy decreased.

Now we can find final expression of the corrected binding energy per atom:

$$E_b = E_{b0} + E_e = \frac{1}{2n}\sum_{N=1}^{N=n}\left(\varepsilon_b C_N - \varepsilon_e Z_N \sum_{N'=1}^{N'=C_N} Z_{N'}\right). \qquad (4)$$

Calculated binding energies for ground-state isomers are presented in the **Table 1**.

Theoretically obtained $E_e - n$ dependence, in general, correlates with experimental cluster-ion intensity dependences form its mass. However main maximum is slightly shifted toward smaller clusters. Such discrepancies may be related to clusters charge – we have calculated binding energy per atom for neutral species, not positive ions as in experiment presented in **Figure 2** .

Conclusions

Studying the boron vapor has shown that, it mainly consists of small (quasi)planar clusters. Boron atoms in nonequivalent sites possess different effective charges. It leads to the nonzero dipole moment for asymmetric species. Binding energy per atom for small boron (quasi)planar clusters are calculated based on quasi-classical B–B interatomic pair potential and taking into account the corrections related to electrostatic interactions between effective atomic charges. This value is found to be correlated with clusters formation probabilities.

Acknowledgement

One of the Authors, Levan Chkhartishvili, is thankful to the Shota Rustaveli National Science Foundation (Georgia) for supporting his participation in ICANM 2015 to present this paper.

References

1. R. Becker, L. Chkhartishvili, P. Martin, Boron, the New Graphene? Vac. Technol. & Coat., 2015, 16, 4, 38-44.
2. Ch. Feldman, K. Moorjani, N. Blum. Mass-spectrometry and optical absorption of boron amorphous films. In: Boron. Obtaining, Structure, and Properties. 1974, Moscow, Nauka, 130-138.
3. W. R. M. Graham, W. Weltner. B atoms, B_2 and H_2BO molecules: ESR and optical spectra at 4 °K. J. Chem. Phys., 1976, 65, 4, 1516-1521.
4. M. Dupuis, B. Liu. The ground electronic state of B_2. J. Chem. Phys., 1978, 68, 6, 2902-2910.
5. I. Carmichael. Ab initio calculation of the hyperfine coupling constants in B_2. J. Chem. Phys., 1989, 91, 2, 1072-1178.
6. Bruna, P.J., Wright, J.S. (1989) Strongly Bound Multiply Excited States of B_2^+ and B_2. J. Chem. Phys. 91(2):1126-1136.
7. P. J. Bruna, J. S. Wright. Theoretical study of the ionization potentials of boron dimer. J. Phys. Chem., 1990, 94, 5, 1774-1781.
8. P. W. Deutsch, L. A. Curtiss, J. A Pople. Boron dimer: Dissociation energy and ionization potentials. Chem. Phys. Lett., 1990, 174, 1, 33-36.
9. S. R. Langhoff, Ch. W. Bauschlicher. Theoretical study of the spectroscopy of B_2. J. Chem. Phys. , 1991, 95, 8, 5882-5888.
10. K. Hald, P. Jorgensen, J. Olsen, M. Jaszunski. An analysis and implementation of a general coupled cluster approach to excitation energies with application to the B_2 molecule. J. Chem. Phys., 2001, 115, 2, 671-679.
11. J. M. L. Martin, J. P. Francois, R. Gijbels. Ab Initio Study of Boron, Nitrogen, and Boron–Nitrogen Clusters. I. Isomers and thermochemistry of B_3, B_2N, BN_2, and N_3. J. Chem. Phys., 1989, 90, 11, 6469-6485.
12. R. Hernandez, J. Simons. Electronic energies, geometries, and vibrational frequencies of the ground and low-lying excited states of the boron trimer. J. Chem. Phys., 1991, 94, 4, 2961-2967.
13. B. Fernandez, P. Jorgensen, J. Simons. Interpretation of the hyperfine coupling constants of the boron trimer in rare-gas matrices. J. Chem. Phys., 1993, 98, 4, 3060-3065.
14. J. M. L. Martin, J. P. Francois, R. Gijbels. Potential energy surface of B_4 and total atomization energies of B_2, B_3, and B_4. Chem. Phys. Lett., 1992, 189, 6, 529-536.

15. H.-J. Zhai, L.-Sh. Wang, A. N. Alexandrova, A. I. Boldyrev, V. G. Zakrzewski. Photoelectron spectroscopy and ab initio study of B_3^- and B_4^- anions and their neutrals. J. Phys. Chem. A, 2003, 107 ,44, 9319-9328.
16. H.-J. Zhai, L.-Sh. Wang, A. N. Alexandrova, A. I. Boldyrev. Electronic sstructure and chemical bonding of B_5^- and B_5 by photoelectron spectroscopy and ab initio calculations. J. Chem. Phys. 2002, 117 ,17, 7917-7924.
17. Q. Sh. Li, H. W. Jin. Structure and stability of B_5, B_5^+, and B_5^- clusters. J. Phys. Chem. A, 2002, 106, 30, 7042-7047.
18. A. N. Alexandrova, A. I. Boldyrev, H.-J. Zhai, L.-Sh. Wang, E. Steiner, P. W. Fowler. Structure and bonding in B_6^- and B_6: Planarity and antiaromaticity. J. Phys. Chem. A, 2003, 107, 9, 1359-1369.
19. A. N. Alexandrova, A. I. Boldyrev, H.-J. Zhai, L.-Sh. Wang. Electronic structure, isomerism, and chemical bonding in B_7^- and B_7. J. Phys. Chem. A, 2004, 108, 16, 3509-3517.
20. P.-L. Cao, W. Zhao, B.-X. Li, B. Song, X.-Y. Zhou. A full-potential linear-Muffin-Tin-Orbital molecular-dynamics study of B_7, B_{10} and B_{13} clusters. J. Phys. Cond. Matter, 2001) 13, 22, 5065-5076.
21. L. Hanley, S. L. Anderson. Production and collision-induced dissociation of small boron cluster ions. J. Phys. Chem .,1987, 91, 20, 5161-5163.
22. H. Kato, E. Tanaka. Stabilities of small Be_n and B_n clusters ($4 \le n \le 8$) by vibrational analysis. J. Comput. Chem., 1991, 12, 9, 1097-1109.
23. A. K. Ray, I. A. Howard, K. M. Kanal. Structure and binding in small neutral and cationic boron clusters. Phys. Rev. B, 1992, 45, 24, 14247-14255.
24. H.-J. Zhai, A. N. Alexandrova, K. A. Birch, A. I. Boldyrev, L. Sh. Wang. Hepta- and octa-coordinate boron in molecular wheels of eight- and nine-atom boron clusters: Observation and confirmation. Angew. Chem. Int. Ed., 2003, 42, 48, 6004-6008.
25. M. L. Drummond, V. Meunier, B. G. Sumpter. Structure and stability of small boron and boron oxide clusters. J. Phys. Chem. A, 2007, 111, 28, 6539-6551.
26. H. Kato, K. Yamashita, K. Morokuma. Ab initio MO study of neutral and cationic boron clusters. Chem. Phys. Lett., 1992, 190, 3-4, 361-366.
27. M. Atis, C. Ozdogan, Z. B. Guvenc. Structure and energetic of B_n ($n = 2-12$) clusters: Electronic structure calculations. Int. J. Quan. Chem., 2007, 107, 3, 729-744.
28. H. C. Longuet–Higgins, M. V. de Roberts. The electronic structure of an icosahedron of boron atoms. Proc. Roy. Soc. A, 1955 ,230, 1180, 110-119.
29. N. E., Solov'ev, E. M. Averbakh, Ya. A. Ugaj. Icosahedron electron energy levels in α-rhombohedral boron. Phys. Solid State, 1984, 26, 1, 195-199.
30. S. Lee, D. M. Bylander, L. Kleinman. Bands and bonds of B_{12}. Phys. Rev. B, 1990, 42, 2, 1316-1320.
31. Ch. L. Beckel, J. P. Vaughan. Vibrations of regular boron icosahedra. AIP Conf. Proc., 1986, 140, 305-311.
32. H. Werheit, U. Kuhlmann. Electron–phonon interaction in B_{12} icosahedra. Solid State Commun., 1993, 88, 6, 421-425.

33. K. Shirai, S. Conda. Polar Vibrations and the effective charges of the icosahedral boron solid. J. Phys. & Chem. Solids, 1996, 57, 1, 109-123.
34. M. Yamaguchi, Y. Ohishi, S. Hosoi, K. Soga, K. Kimura. Metallic–covalent bonding conversion in boron icosahedral cluster solids studied using electron localizability indicator. J. Phys. Conf. Ser., 2009, 176, 012027, 1-10.
35. L. Hanley, J. L. Whitten, S. L. Anderson. Collision-induced dissociation and ab initio studies of boron cluster ions: Determination of structures and stabilities. J. Phys. Chem., 1988, 92, 20, 5803-5812.
36. L. Hanley, J. L. Whitten, S. L. Anderson. Collision-induced dissociation and ab initio studies of boron cluster ions: Determination of structures and stabilities [Erratum to document cited in CA109(18):156723t]. J. Phys. Chem., 1990, 94, 5, 2218-2218.
37. R. Kawai, J. H. Weare. Anomalous stability of B_{13}^+ clusters. Chem. Phys. Lett., 1992, 191, 3-4, 311-314.
38. H. Kato, K. Yamashita, K. Morokuma. Ab initio study of neutral and cationic B_{12} and B_{13} clusters. Bull. Chem. Soc. Jpn., 1993, 66, 11, 3358-3361.
39. F. L. Gu, X. Yang, A.-Ch. Tang, H. Jiao, P. von R. Schleyer. Structure and stability of B_{13}^+ clusters. J. Comput. Chem., 1998, 19, 2, 203-214.
40. J. E. Fowler, J. M. Ugalde. The curiously stable B_{13}^+ cluster and its neutral and anionic counterparts: the advantages of planarity. J. Phys. Chem. A, 2000, 104, 2, 397-403.
41. J.-I. Aihara. B_{13}^+ is highly aromatic. J. Phys. Chem. A, 2001, 105, 22, 5486-5489.
42. T. B. Tai, D. J. Grant, M. T. Nguyen, D. A. Dixon. Thermochemistry and electronic structure of small boron clusters (B_n, $n = 5-13$) and their anions. J. Phys. Chem. A, 2010, 114, 2, 994-1007.
43. N. Akman, M. Tas, C. Ozdogan, I. Boustani. Ionization energies, coulomb explosion, fragmentation, geometric, and electronic structures of multicharged boron clusters B_n ($n = 2-13$). Phys. Rev. B, 2011, 84, 075463, 1-10.
44. Q. Sh. Li, F. L. Gu, A. C. Tang. Quantum chemistry study on B_{14}, B_{14}^{2-}, and $B_{14}H_{14}^{2-}$. Int. J. Quan. Chem., 1994, 50, 3, 173-179.
45. I. Boustani. Systematic LSD investigation on cationic boron clusters: B_n^+ ($n = 2-14$). Int. J. Quan. Chem., 1994, 52, 4, 1081-1111.
46. I. Boustani. A comparative study of ab initio SCF–CI and DFT. example of small boron Clusters. Chem. Phys. Lett., 1995, 233, 3, 273-278.
47. I. Boustani. Structure and stability of small boron clusters. A density functional theoretical study. Chem. Phys. Lett., 1995, 240, 1-3, 135-140.
48. A. Ricca, Ch. W. Bauschlicher Jr. The structure and stability of B_n^+ clusters. Chem. Phys., 1996, 208, 2, 233-242.
49. I. Boustani. New convex and spherical structures of bare boron clusters. J. Solid State Chem., 1997, 133, 1, 182-189.
50. I. Boustani. New quasi-planar surfaces of bare boron. Surf. Sci., 1997, 370, 2-3, 355-363.
51. I. Boustani. Systematic ab initio investigation of bare boron clusters: determination of the geometry and electronic structures of B_n ($n = 2-14$). Phys. Rev. B, 1997, 55, 24, 16426-16438.

52. E. Oger, N. Crawford, R. Kelting, P. Weis, M. Kappes, R. Ahlrichs. Boron cluster cations: transition from planar to cylindrical structures. Angew. Chem. Int. E., 2007, 46, 44, 8503-8506.
53. A. P. Sergeeva, D. Yu. Zubarev, H.-J. Zhai, A. I. Boldyrev, L.-Sh. Wang. A photoelectron spectroscopic and theoretical study of B_{16}^- and B_{16}^{2-}: An all-boron naphthalene. J. Am. Chem. Soc., 2008, 130, 23, 7244-7246.
54. W. Huang, A. P. Sergeeva, H.-J. Zhai, B. B. Averkiev, L.-Sh. Wang, A. I. Boldyrev. A Concentric planar doubly π-aromatic B_{19}^- cluster. Nat. Chem., 2010, 2, 3, 202-206.
55. B. Kiran, S. Bulusu, H.-J. Zhai, S. Yoo, X. Ch. Zeng, L.-Sh. Wang. Planar-to-tubular structural transition in boron clusters: B_{20} as the embryo of single-walled boron nanotubes. Proc. Natl. Acad. Sci. USA, 2005, 102, 4, 961-964.
56. W. An, S. Bulusu, Y. Gao, X. C. Zeng. Relative stability of planar versus double-ring tubular isomers of neutral and anionic boron clusters B_{20} and B_{20}^-. J. Chem. Phys., 2006, 124, 154310, 1-6.
57. L.-Sh. Wang. Probing the electronic structure and chemical bonding of boron clusters using photoelectron spectroscopy of size-selected cluster anions. In: 16th Int. Symp. Boron, Borides & Rel. Mater., 2008, Matsue, KM, 61-61.
58. I. Boustani, A. Quandt, E. Hernandez, A. Rubio. New boron based nanostructured materials. J. Chem. Phys., 1999, 110, 6, 3178-3185.
59. S. Chacko, D. G. Kanhere, I. Boustani. Ab initio density functional investigation of B_{24} clusters: rings, tubes, planes, and cages. Phys. Rev. B ,2003, 68, 035414, 1-11.
60. I. Boustani, A. Rubio, J. A. Alonso. Ab initio study of B_{32} clusters: Competition between spherical, quasiplanar and tubular isomers. Chem. Phys. Lett., 1999, 311, 1, 21-28.
61. S. J. la Placa, P. A. Roland, J. J. Wynne. Boron clusters (B_n, $n = 2-52$) produced by laser ablation of hexagonal boron nitride. Chem. Phys. Lett., 1992, 190, 3-4, 163-168.
62. I. Boustani. Structural transitions and properties of boron nanoclusters. In: 17th Int. Symp. Boron, Borides & Rel. Mater., 2011, Ankara:, BKM, 49-49.
63. S.-J. Xu, J. M. Nilles, D. Radisic, W.-J. Zheng, S. Stokes, K. H. Bowen, R. C. Becker, I. Boustani. Boron cluster anions containing multiple B_{12} icosahedra. Chem. Phys. Lett., 2003, 379, 3-4, 282-286.
64. A.-Ch. Tang, Q.-Sh. Li, Ch.-W. Liu, J. Li. Symmetrical clusters of carbon and boron. Chem. Phys. Lett., 1993, 201, 5-6, 465-469.
65. I. Boustani, A. Quandt. Boron in ab initio calculations. Comput. Mater. Sci., 1998, 11, 1, 132-137.
66. H.-J. Zhai, B. Kiran, J. Li, L.-Sh. Wang. Hydrocarbon analogues of boron clusters – Planarity, aromaticity and antiaromaticity. Nat. Mater., 2003, 2, 12, 827-833.
67. I. Boustani. Theoretical prediction and experimental observation of boron quasiplanar clusters and single-wall nanotubes. In: 15th Int. Symp. Boron, Borides & Rel. Mater., 2005, Hamburg, UH, 41-41.
68. A. N. Alexandrova, A. I. Boldyrev, H-J. Zhai, L.-Sh. Wang. All-boron aromatic clusters as potential new inorganic ligands and building blocks in chemistry. Coord. Chem. Rev., 2006, 250, 21-22, 2811-2866.

69. Z. A. Piazza, H.-Sh. Hu, W.-L. Li, Y.-F. Zhao, J. Li, L.-Sh. Wang. Planar hexagonal B_{36} as a potential basis for extended single-atom layer boron sheets. Nat. Commun., 2014, 5, 3113, 1-15.
70. N. Vast, S. Bernard, G. Zerah. Structural and electronic properties of liquid boron from a molecular-dynamics simulation. Phys. Rev. B, 1995, 52, 6, 4123-4130.
71. Sh. Krishnan, S. Ansell, J. J. Felten, K. J. Volin, D. L. Price. Structure of liquid boron. Phys. Rev. Lett., 1998, 81, 3, 586-589.
72. D. L. Price, A. Alatas, L. Hennet, N. Jakse, Sh. Krishnan, A. Pasturel, I. Pozdnyakova, M.-L. Saboungi, A. Said, R. Scheunemann, W. Schirmacher, H. Sinn. Liquid boron: X-ray measurements and ab initio molecular dynamics simulations. Phys. Rev. B, 2009, 79, 134201, 1-5.
73. R. C. Becker. Method for generating a boron vapor. U.S. Patent: #5,861,630, 1999.
74. R. Becker, L. Chkhartishvili, R. Avci, I. Murusidze, O. Tsagareishvili, N. Maisuradze, "Metallic" boron nitride. Eur. Chem. Bull., 2015, 4, 1-3, 8-23.
75. R. Becker, L. Chkhartishvili. On possible nature of metallic conductance of boron–nitrogen compounds. In: Abs. 3rd Int. Conf. "Nanotechnologies". 2014, Tbilisi, Publ. House Tech. Univ., 13-14.
76. I. Boustani, R. Becker. Boron clusters, single- and multi-walled nanotubes: Theoretical prediction and experimental observation. In: Proc. 9th Ann. Nanotechnol. Conf. & Trade Show. 2006, Boston, NSTI, MO 60.802.
77. L. Chkhartishvili. Quasi-Classical Theory of Substance Ground State. 2004, Tbilisi, Tech. Univ. Press.
78. L. Chkhartishvili, D. Lezhava, O. Tsagareishvili, D. Gulua. Ground-state parameters of diatomic molecules B_2, BC, BN and BO. Trans, Acad. MIA Georg., 1999, 1, 295-300.
79. L. Chkhartishvili, D. Lezhava, O. Tsagareishvili. Quasi-classical determination of electronic energies and vibration frequencies in boron compounds. J. Solid State Chem., 2000, 154, 1, 148-152.
80. L. Chkhartishvili. Molar binding energy of the boron nanosystems. In: Proc. 4th Int. Boron Symp. 2009, Eskisehir, Osmangazi Univ. Press, 153-160.
81. L. Chkhartishvili. On quasi-classical estimations of boron nanotubes ground-state parameters. J. Phys. Conf. Ser., 2009, 176, 012013, 1-9.
82. L. Chkhartishvili. Geometrical models for bare boron nanotubes. In: Physics, Chemistry and Applications of Nanostructures. 2011, Singapore: World Scientific, 118-121.
83. L. Chkhartishvili. Nanotubular boron: Ground-state estimates. In: New Developments in Materials Science. 2011, New York, Nova Sci. Publ., Ch.8, 67-80.
84. L. S. Chkhartishvili, D. L. Gabunia, O. A. Tsagareishvili. Estimation of the isotopic effect on the melting parameters of boron. Inorg. Mater., 2007, 43, 6, 594-596.
85. L. S. Chkhartishvili, D. L. Gabunia, O. A. Tsagareishvili. Effect of the isotopic composition on the lattice parameter of boron. Powder Metall. & Met. Ceram., 2008, 47(9-10):616-621.
86. L. Chkhartishvili. Isotopic effects of boron (Review). Trends Inorg. Chem., 2009, 11, 105-167.

87. D. Gabunia, O. Tsagareishvili, L. Chkhartishvili, L. Gabunia. Isotopic composition dependences of lattice constant and thermal expansion of β-rhombohedral boron. J. Phys. Conf. Ser., 2009, 176, 012022, 1-10.
88. L. Chkhartishvili, O. Tsagareishvili, D. Gabunia. Isotopic expansion of boron. J. Metall. Eng., 2014, 3, 3, 97-103.